

Supporting Information

Injectable, thermo-sensitive and self-adhesive supramolecular hydrogels built from binary herbal small molecules towards reusable antibacterial coatings

*Zhibin Dong,^a Fengjun Ma,^a Xiaocen Wei,^a Linlin Zhang,^a Yongling Ding,^b Lei Shi,^{*a} Chen Chen^a, Yuxia Ma,^{*a} Yuning Ma^{*a}*

*Corresponding authors: 60230082@sducm.edu.cn; myxia1976@163.com; myning0405@163.com.

^a Key Laboratory of New Material Research Institute, Department of Acupuncture-Moxibustion and Tuina, Institute of Pharmacy, Shandong University of Traditional Chinese Medicine, Jinan 250355, P.R. China

^b School of Transportation Civil Engineering, Shandong Jiaotong University, Jinan, 250357, P.R. China

Table S1. The detailed preparation conditions of the herbal hydrogels.

Hydrogel	Monomer A	Monomer B	Heating time (h)	Gelation time (min)
EGCG-St	EGCG (1.83 g, 2.0 M)	St (4.02 g, 2.5 M)	18	10
PC-St	PC (1.19 g, 1.0 M)	St (4.02 g, 2.5 M)	25	10
TP-St	TP (2.80 g, 5.0 M)	St (4.02 g, 2.5 M)	15	10
TA-RA	TA (3.40 g, 1.0 M)	RA (2.90 g, 1.5 M)	10	10

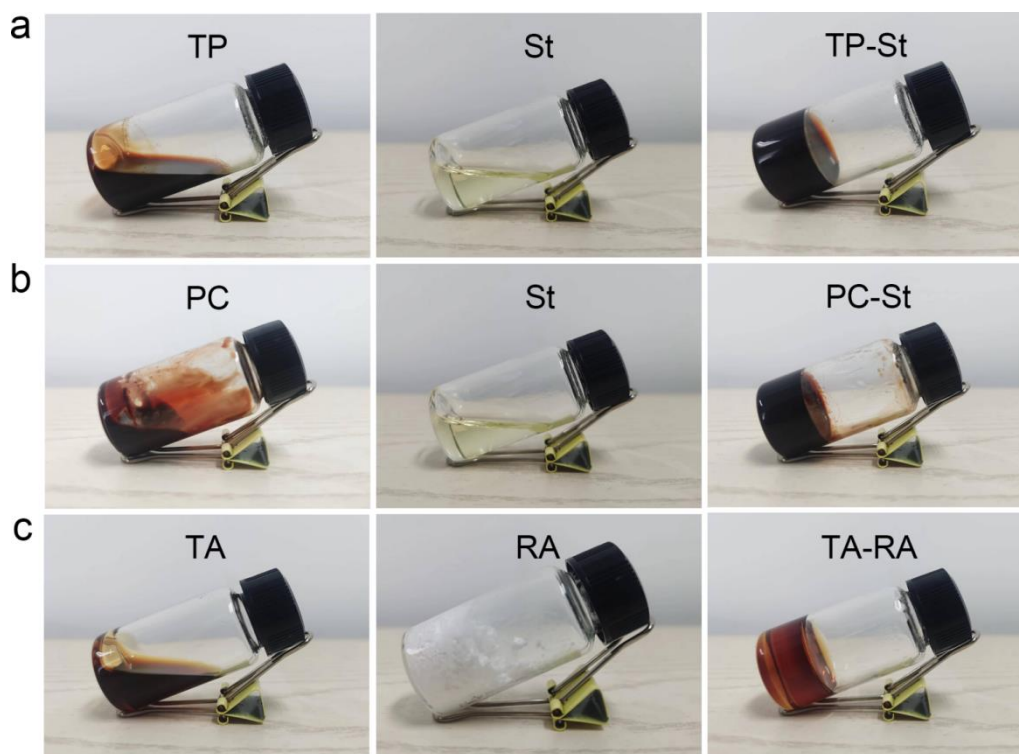


Figure S1. Photos showing the states of (a) TP-St, (b) PC-St, and (c) TA-RA hydrogels and their corresponding monomers.

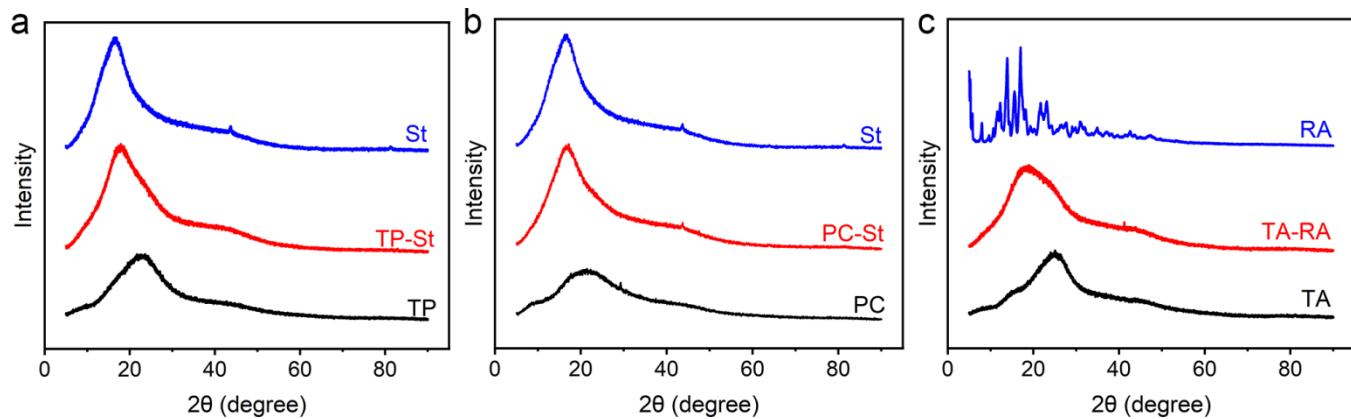


Figure S2. XRD patterns of the lyophilized (a) TP-St, (b) PC-St, and (c) TA-RA hydrogels and their corresponding monomers.



Figure S3. SEM images of the lyophilized (a) TP-St, (b) PC-St, and (c) TA-RA hydrogels.

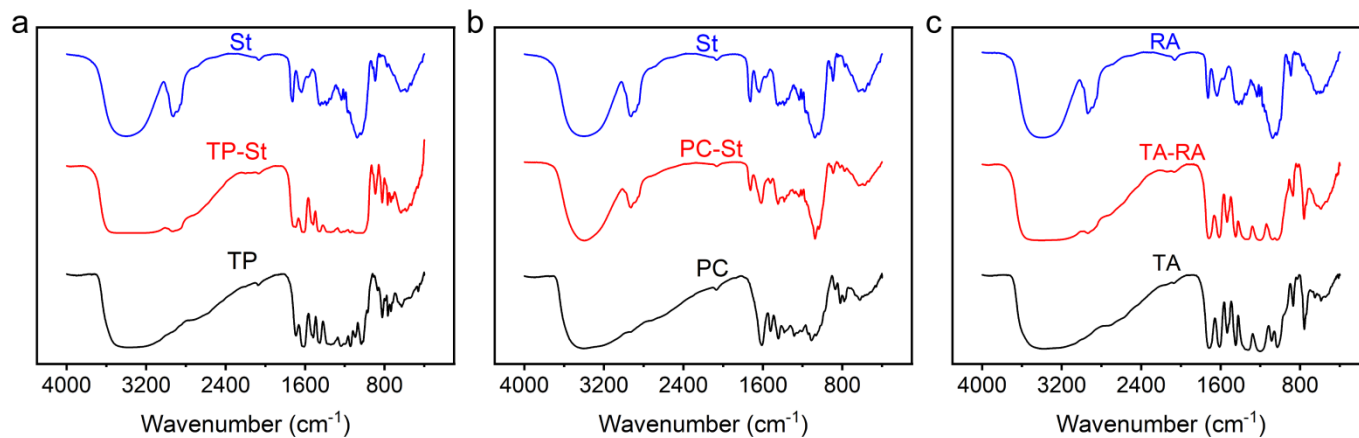


Figure S4. FT-IR spectra of the lyophilized (a) TP-St, (b) PC-St, and (c) TA-RA hydrogels and their corresponding monomers.

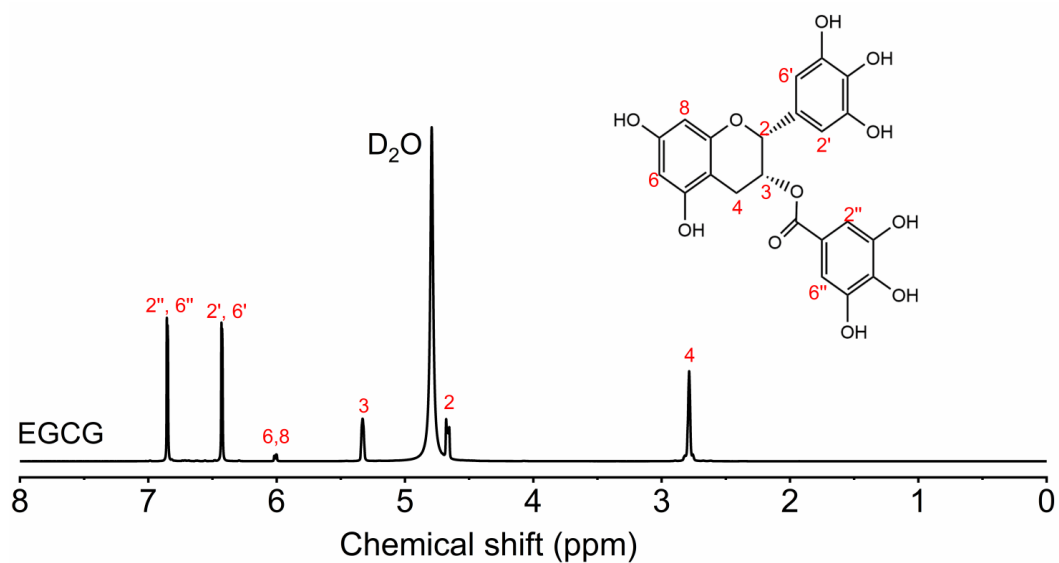


Figure S5. ^1H NMR spectrum of EGCG in D_2O .

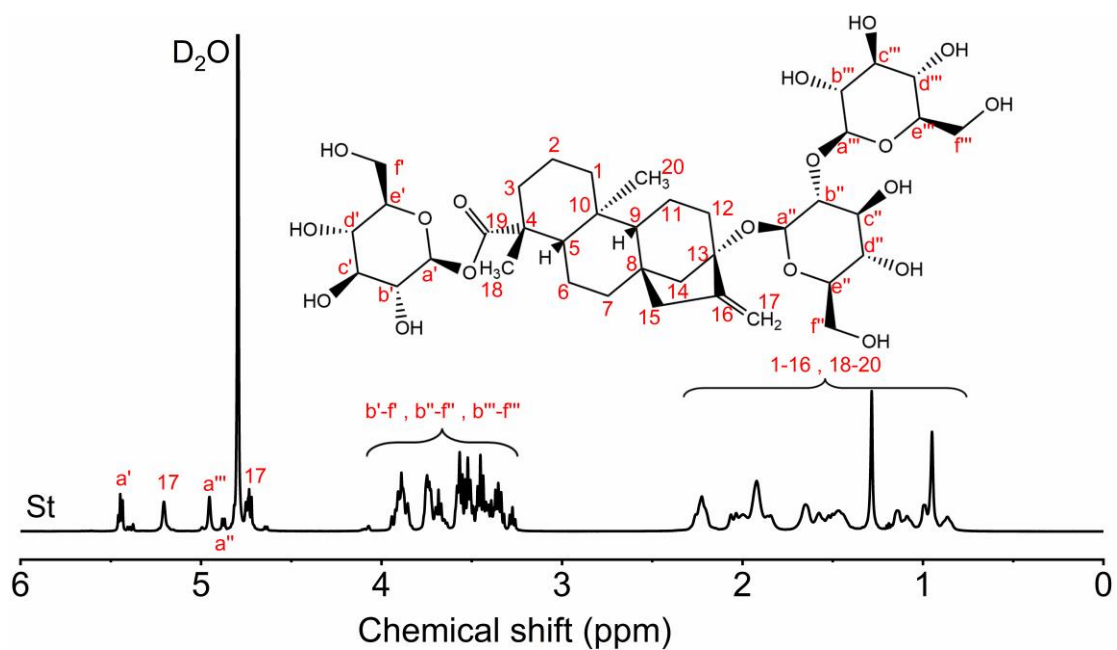


Figure S6. ^1H NMR spectrum of St in D_2O .

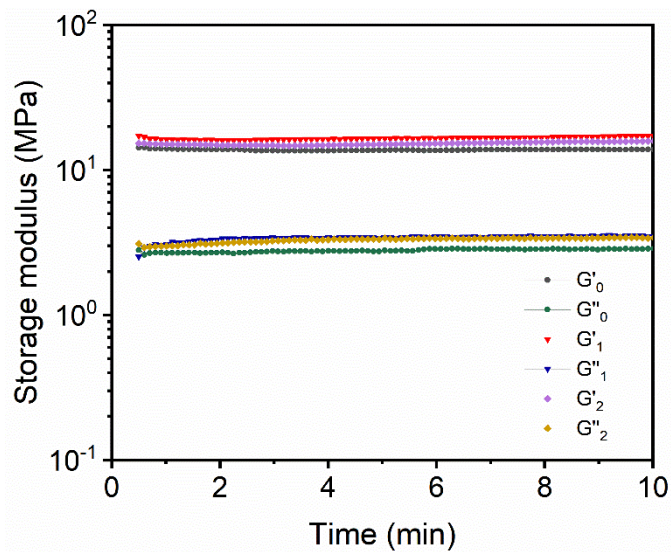


Figure S7. The G' and G'' values of freshly prepared EGCG-St hydrogel before and after two heating-cooling processes.

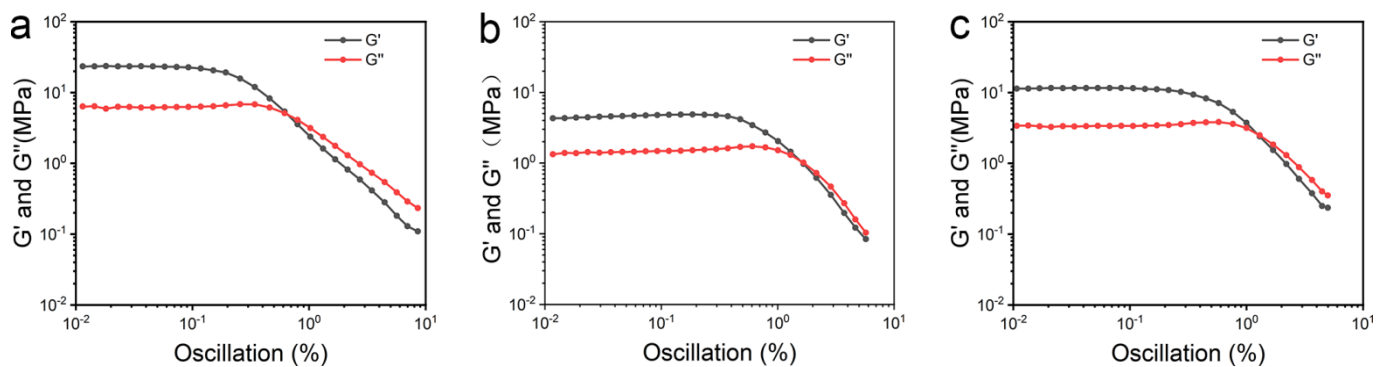


Figure S8. Strain-dependent oscillatory shear rheologies of (a) TP-St, (b) PC-St, and (c) TA-RA hydrogels with a fixed frequency of 10 rad s^{-1} .

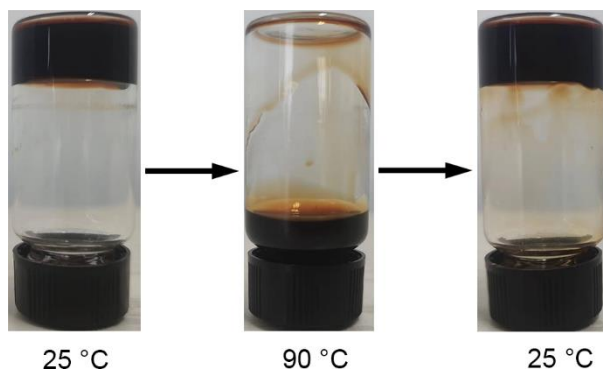


Figure S9. Photos showing the reversible thermal-responsive behavior of TP-St hydrogel.

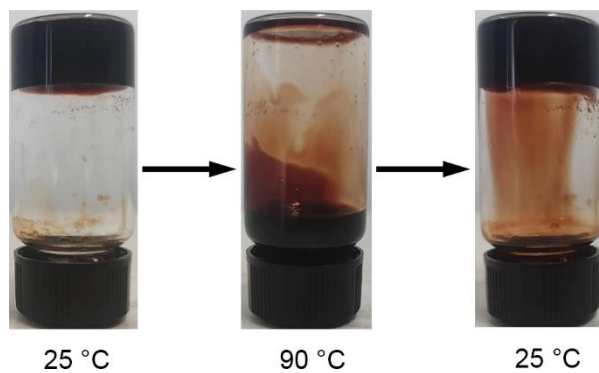


Figure S10. Photos showing the reversible thermal-responsive behavior of PC-St hydrogel.

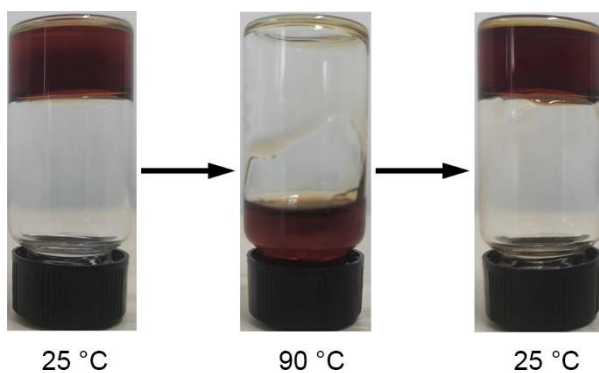


Figure S11. Photos showing the reversible thermal-responsive behavior of TA-RA hydrogel.



Figure S12. Photo demonstrating the injectability of EGCG-St hydrogel using a syringe.

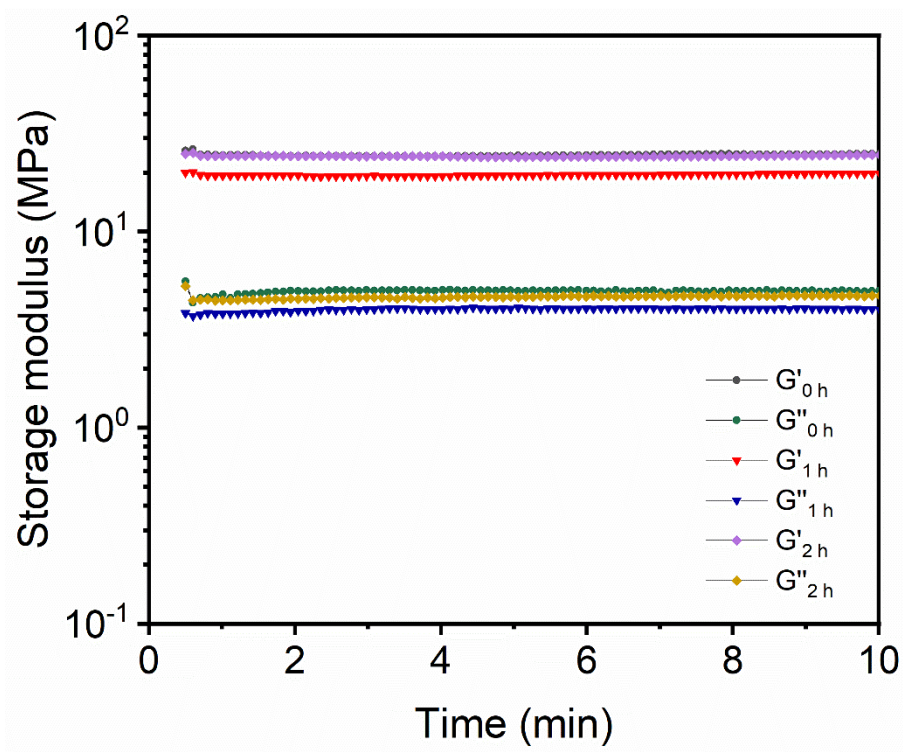


Figure S13. The G' and G'' values of EGCG-St hydrogel after being injected through a syringe needle for 1h and 2h, and those of freshly prepared EGCG-St hydrogel.